

The effect of the chiral chemical potential on the chiral phase transition in the NJL model with different regularization schemes

Lang Yu^{1,2,*}, Hao Liu^{2,†} and Mei Huang^{2,3‡}

¹ *Center of Theoretical Physics and College of Physics, Jilin University, Changchun, 130012, China*

² *Institute of High Energy Physics, Chinese Academy of Sciences, Beijing 100049, China and*

³ *Theoretical Physics Center for Science Facilities,
Chinese Academy of Sciences, Beijing 100049, China*

(Dated: July 24, 2018)

We study the chiral phase transition in the presence of the chiral chemical potential μ_5 using the two-flavor Nambu–Jona-Lasinio model. In particular, we analyze the reason why one can obtain two opposite behaviors of the chiral critical temperature as a function of μ_5 in the framework of different regularization schemes. We compare the modifications of the chiral condensate and the critical temperature due to μ_5 in different regularization schemes, analytically and numerically. Finally, we find that, for the conventional hard-cutoff regularization scheme, the increasing dependence of the critical temperature on the chiral chemical potential is an artifact, which is caused by the fact that it does not include complete contribution from the thermal fluctuations. When the thermal contribution is fully taken into account, the chiral critical temperature should decrease with μ_5 .

PACS numbers: 12.38.Aw, 12.38.Mh

I. INTRODUCTION

Quantum chromodynamics (QCD), the theory of strong interactions, is expected to explore the phase structure and phase diagram of QCD. Such research on the QCD vacuum and matter is very important to get a deeper understanding of the early Universe, the compact stars and the phenomena in relativistic heavy ion collision experiments (e.g. the quark-gluon plasma), and so on. One of the most intriguing fundamental features of QCD is spontaneous breakdown of chiral symmetry. The chiral symmetry breaking and restoration can be characteristically described in terms of the chiral condensate, which is the order parameter of chiral symmetry breaking in the chiral limit (an approximate order parameter when the current quark mass is small). As a consequence, it is crucial to make theoretical investigations on the behavior of the chiral condensate, in order to comprehend the chiral phase transition and the nonperturbative properties of the strong interactions.

It is well known that QCD at zero and low temperatures has a nontrivial topological structure due to the existence of certain gluon configuration, i.e. instantons [1–3], which can be assigned an integer-valued topological winding number. And the infrared instanton structure is believed to explain chiral symmetry breaking of the QCD vacuum [4]. However, at present, experimental evidence for the existence of such topological gluon configurations can only be found indirectly from the meson spectrum [5, 6].

When at high temperatures, e.g. in the quark-gluon plasma, which is a phase of extremely hot QCD matter

created in heavy ion collisions, a copious production of another kind of topological gluon configurations (i.e. the QCD sphalerons) is expected [7–12]. The topologically nontrivial sphaleron transitions can induce chirality imbalance, and thus lead to the breaking of the parity (\mathcal{P}) and charge-parity (\mathcal{CP}) symmetry in the hot plasma via the axial anomaly of QCD. Since there is no direct \mathcal{P} and \mathcal{CP} violation in QCD, chirality imbalance can only be produced locally and vanishes on average. It means that the probability to generate a local domain with a positive winding number Q_W is the same as the probability to generate a local domain with a negative winding number $-Q_W$. And such local chirality imbalance can give rise to local \mathcal{P} - and \mathcal{CP} -odd domains in the quark-gluon plasma phase of QCD. Unlike the instanton transitions, which are thermally suppressed [7–12], the sphaleron transitions are not suppressed and so the gluon configurations with nonzero winding number can be produced with relatively high probability [13–17]. Therefore, the quark gluon plasma, created by the heavy ion collisions, provides the best platform to probe direct experimental evidence for the existence of nontrivial topological gluon configurations, as well as local \mathcal{P} and \mathcal{CP} violation.

On the other hand, it has been suggested that strong magnetic fields can be generated in noncentral heavy ion collisions [18–21]. It was proposed that the interplay between the local chirality imbalance and the magnetic field will induce a current along the direction of the magnetic field, which is called chiral magnetic effect (CME) [22, 23, 38]. This effect leads to a separation of positive and negative electric charges with respect to the reaction plane of the heavy ion collisions. The recent observation of charge azimuthal correlations at RHIC and LHC [25–27] possibly resulted from the CME, which is a direct consequence of nontrivial topological gluon configurations in the strong magnetic field background. Moreover, Concerning the influence of the magnetic field on

* yulang@jlu.edu.cn

† haoliu@mail.ihep.ac.cn

‡ huangm@mail.ihep.ac.cn

the QCD phase diagram, there have been many other interesting phenomena besides the CME, such as magnetic catalysis [28–30], inverse magnetic catalysis [31, 32], and vacuum superconductivity [33, 34]. In particular, the local chirality imbalance induced by the nontrivial topological gluon configuration is also one of possible mechanisms trying to explain the inverse magnetic catalysis effect [35–37].

Since local chirality imbalance is expected to be produced in the quark gluon plasma, it is of great interest to investigate the effects of the chirality imbalance on the phase structure and phase transition of QCD. In order to treat the induced chirality imbalance, a chiral chemical potential μ_5 can be introduced, which creates a difference between the number of right- and left-handed quarks. The chiral chemical potential can be related to the θ angle of strong interactions as follows [23]:

$$\mu_5 = \frac{1}{2N_f} \frac{\partial \theta}{\partial t}, \quad (1)$$

where t is the time coordinate and N_f is the number of the light flavors.

In this article, we will focus on studying the effects of the chiral chemical potential μ_5 on the chiral phase transition in the framework of the two-flavor Nambu–Jona-Lasinio (NJL) model. Actually, it has been studied by using some effective models of QCD [38–41], Dyson-Schwinger equations (DSEs) [42, 43] and lattice QCD simulations [44] in recent years, but they do not reach an agreement on the modification of the chiral transition temperature by the chiral chemical potential μ_5 . The results of most effective models in Refs. [38–40] show that the critical temperature of the chiral phase transition decreases with μ_5 , whereas the results of the NJL model in Ref. [41], DSEs in Ref. [43], and lattice QCD in Ref. [44] show a completely different dependence of the critical temperature on μ_5 , i.e. increasing with μ_5 . Since we have no idea about the details of computations in DSEs [43] and lattice QCD [44], we will not discuss them in this paper. It is very surprising that the results in Ref. [38, 40] are in contradiction to those in Ref. [41], although these two papers use the same NJL model. The only difference between them is the regularization scheme. Hence, at the same time, we will investigate how the regularization schemes, at least in the NJL model, influence the effects of the chiral chemical potential on the chiral condensate and the chiral critical temperature of QCD. This is the main scope of this article. Furthermore, in Refs. [38–40] the chiral phase transition becomes first order at some critical value of the chiral chemical potential, while in Ref. [41] as well as [43, 44], there is no such a behavior and the order of the phase transition always stays the same. We find that the order of the transition also depends on the regularization scheme in the NJL model after doing numerical calculations.

The paper is organized as follows. In Sec. II, we give a general description of the NJL model with introducing the chiral chemical potential. In Sec. III, we perform a

systematic analysis of the effects of the chiral chemical potential on the chiral condensate and the chiral critical temperature for different regularization schemes in the NJL model, analytically and numerically. Finally, we present our conclusions in Sec. IV.

II. MODEL

The Lagrangian density of our model is given by

$$\mathcal{L} = \bar{\psi} (i\gamma_\mu \partial^\mu + \mu_5 \gamma^0 \gamma^5) \psi + G_S \left[(\bar{\psi}\psi)^2 + (\bar{\psi}i\gamma^5 \boldsymbol{\tau}\psi)^2 \right]. \quad (2)$$

In the above equation, ψ corresponds to the quark field of two light flavors u and d . G_S is the coupling constants with respect to the scalar and pseudoscalar channels. For simplicity, we will just work in the chiral limit throughout the paper, which gives no ambiguity for the definition of the chiral critical temperature. In addition, unlike Ref. [38], we work at zero magnetic field in this paper, so that we can avoid considering inverse magnetic catalysis, whose underlying physics is still under debate at present.

At the mean field level, the corresponding Lagrangian from Eq. (2) can be given by the following formula:

$$\mathcal{L} = -\frac{\sigma^2}{4G_S} + \bar{\psi} (i\gamma_\mu \partial^\mu - \sigma + \mu_5 \gamma^0 \gamma^5) \psi, \quad (3)$$

where $\sigma = -2G_S \langle \bar{\psi}\psi \rangle$ is the dynamical quark mass.

Thus, the thermodynamical potentials Ω^S with soft cutoff and Ω^H with hard cutoff are given by, respectively,

$$\begin{aligned} \Omega^S &= \frac{\sigma^2}{4G_S} - N_c N_f \sum_{s=\pm} \int \frac{d^3p}{(2\pi)^3} f_\Lambda^2(p) \omega_s(p) \\ &\quad - 2N_c N_f T \sum_{s=\pm} \int \frac{d^3p}{(2\pi)^3} \ln(1 + e^{-\beta\omega_s}) \\ &= \frac{\sigma^2}{4G_S} - N_c N_f \sum_{s=\pm} \int_0^\infty \frac{dp}{2\pi^2} f_\Lambda^2(p) p^2 \omega_s \\ &\quad - 2N_c N_f T \sum_{s=\pm} \int_0^\infty \frac{dp}{2\pi^2} p^2 \ln(1 + e^{-\beta\omega_s}), \end{aligned} \quad (4)$$

and

$$\begin{aligned} \Omega^H &= \frac{\sigma^2}{4G_S} - N_c N_f \sum_{s=\pm} \int \frac{d^3p}{(2\pi)^3} \omega_s(p) \\ &\quad - 2N_c N_f T \sum_{s=\pm} \int \frac{d^3p}{(2\pi)^3} \ln(1 + e^{-\beta\omega_s}) \\ &= \frac{\sigma^2}{4G_S} - N_c N_f \sum_{s=\pm} \int_0^\Lambda \frac{dp}{2\pi^2} p^2 \omega_s \\ &\quad - 2N_c N_f T \sum_{s=\pm} \int_0^\Lambda \frac{dp}{2\pi^2} p^2 \ln(1 + e^{-\beta\omega_s}). \end{aligned} \quad (5)$$

where $\omega_s \equiv \omega_s(p) = \sqrt{\sigma^2 + [|\mathbf{p}| + s\mu_5]^2}$, are the eigenvalues of the Dirac operator with spin factors $s = \pm 1$,

and $\beta = 1/T$. To avoid cutoff artifact, following Ref. [38] we use a smooth regularization scheme, labeled as the soft cutoff, by introducing a form factor $f_\Lambda(p)$ to deal with the divergence in the zero-point energy:

$$f_\Lambda(p) = \sqrt{\frac{\Lambda^{2N}}{\Lambda^{2N} + |\mathbf{p}|^{2N}}}, \quad (6)$$

where we take $N = 5$ specifically. In the $N \rightarrow \infty$ limit, the above $f_\Lambda(p)$ (or $f_\Lambda(p)^2$) is reduced to the hard cutoff function $\theta(\Lambda - |\mathbf{p}|)$. Actually, we do not need to introduce a cutoff function for the thermal part of Ω , since Ω_{th} is not divergent at all. However, in the conventional hard-cutoff regularization scheme, the hard cutoff function is always introduced for the thermal part of Ω , which leads to a quite different behavior of the chiral condensate at finite temperature as well as the transition temperature T_c . This will be discussed later. Thus, we introduce a revised hard-cutoff regularization scheme $\Omega^{H'}$ by replacing the thermal part of Ω^H with that of Ω^S :

$$\begin{aligned} \Omega^{H'} &= \frac{\sigma^2}{4G_S} - N_c N_f \int \sum_{s=\pm} \frac{d^3 p}{(2\pi)^3} \omega_s(p) \\ &\quad - 2N_c N_f T \sum_{s=\pm} \int \frac{d^3 p}{(2\pi)^3} \ln(1 + e^{-\beta\omega_s}) \\ &= \frac{\sigma^2}{4G_S} - N_c N_f \sum_{s=\pm} \int_0^\Lambda \frac{dp}{2\pi^2} p^2 \omega_s \\ &\quad - 2N_c N_f T \sum_{s=\pm} \int_0^\infty \frac{dp}{2\pi^2} p^2 \ln(1 + e^{-\beta\omega_s}). \end{aligned} \quad (7)$$

It is natural to predict that the effects of the chiral chemical potential on the chiral condensate and the transition temperature obtained from $\Omega^{H'}$ should be consistent with those obtained from Ω^S . Since we will find that Ω^S and $\Omega^{H/H'}$ give similar results in the QCD vacuum. These points will be discussed and verified in some details in the later section. Therefore, we will just need to show why $\Omega^{H'}$ leads to a result different from Ω^H about the influence of the chiral chemical potential on the transition temperature.

The thermodynamical potential Ω by using either soft cutoff or hard cutoff can be divided into two parts, the vacuum part and the thermal part:

$$\Omega = \Omega_{vac} + \Omega_{th}, \quad (8)$$

where

$$\begin{aligned} \Omega_{vac}^S &= \frac{\sigma^2}{4G_S} - N_c N_f \sum_{s=\pm} \int_0^\infty \frac{dp}{2\pi^2} f_\Lambda^2(p) p^2 \omega_s \\ \Omega_{th}^S &= -2N_c N_f T \sum_{s=\pm} \int_0^\infty \frac{dp}{2\pi^2} p^2 \ln(1 + e^{-\beta\omega_s}), \end{aligned} \quad (9)$$

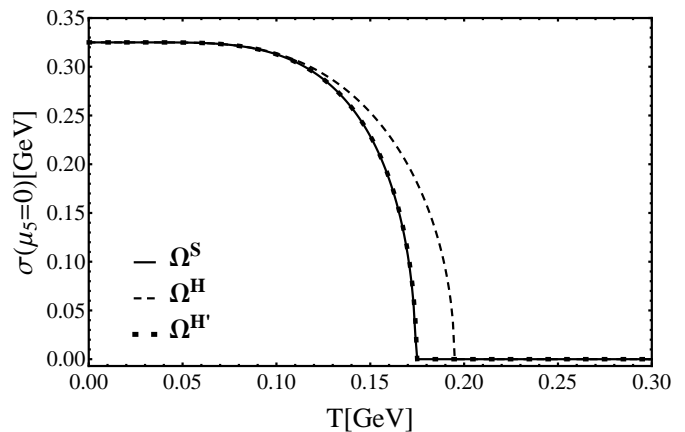


FIG. 1. The dynamical quark mass σ as a function T at $\mu_5 = 0$ for Ω^S , Ω^H and $\Omega^{H'}$.

and

$$\begin{aligned} \Omega_{vac}^{H/H'} &= \frac{\sigma^2}{4G_S} - N_c N_f \sum_{s=\pm} \int_0^{\Lambda/\Lambda} \frac{dp}{2\pi^2} p^2 \omega_s \\ \Omega_{th}^{H/H'} &= -2N_c N_f T \sum_{s=\pm} \int_0^{\Lambda/\infty} \frac{dp}{2\pi^2} p^2 \ln(1 + e^{-\beta\omega_s}), \end{aligned} \quad (10)$$

Now, σ can be determined self-consistently by solving the saddle point equation (the gap equation)

$$\frac{\partial \Omega}{\partial \sigma} = 0. \quad (11)$$

III. CHIRAL PHASE TRANSITION WITH CHIRAL CHEMICAL POTENTIAL

In this section we compare the results on the QCD chiral phase transition at zero and finite chiral chemical potential by using three different regularization schemes, i.e. Ω^S , Ω^H and $\Omega^{H'}$. In this way we analyze the reasons why $\Omega^{H'}$ (or Ω^S) and Ω^H exhibit similar behaviors on the chiral condensate and the transition temperature at zero and low temperatures, but totally different ones at high temperatures.

In addition, our model parameter set is

$$\Lambda = 626.76 \text{ MeV}, \quad G_S \Lambda^2 = 2.02, \quad \text{for } \Omega^S; \quad (12)$$

$$\Lambda = 633.27 \text{ MeV}, \quad G_S \Lambda^2 = 2.19, \quad \text{for } \Omega^H \text{ and } \Omega^{H'} \quad (13)$$

These parameters correspond to $f_\pi = 92.3$ MeV and the constituent quark mass $M = 325$ MeV.

A. Analysis and Results at $\mu_5 = 0$

When at $\mu_5 = 0$, with the help of numerical simulations, we compute the behavior of the dynamical quark

mass σ as a function T for Ω^S , Ω^H and $\Omega^{H'}$, which is shown in Fig. 1. And numerically we find the transition temperature T_c for these three regularization schemes: $T_c^S(\mu_5 = 0) = 174.3$ MeV for Ω^S , $T_c^H(\mu_5 = 0) = 194.9$ MeV for Ω^H , and $T_c^{H'}(\mu_5 = 0) = 174.6$ MeV for $\Omega^{H'}$. Apparently, the results by Ω^S are consistent with those by $\Omega^{H'}$, but the values of T_c and σ near T_c by Ω^H are larger than those by Ω^S and $\Omega^{H'}$.

As we know, at $\mu_5 = 0$, Ω_{vac}^H and $\Omega_{vac}^{H'}$ have the same expressions, and we obtain that

$$\begin{aligned} \Omega_{vac}^{H/H'}(\mu_5 = 0) &= \frac{\sigma^2}{4G_S} - \frac{N_c N_f}{2\pi^2} \times \frac{1}{4} \left[2\Lambda^3 \sqrt{\Lambda^2 + \sigma^2} \right. \\ &\quad \left. + \Lambda \sigma^2 \sqrt{\Lambda^2 + \sigma^2} + \sigma^4 \ln\left(\frac{\sigma}{\Lambda + \sqrt{\Lambda^2 + \sigma^2}}\right) \right] \end{aligned} \quad (14)$$

When $\sigma/\Lambda \rightarrow 0$, we can get

$$\begin{aligned} \Omega_{vac}^{H/H'}(\mu_5 = 0) &\sim \frac{\sigma^2}{4G_S} - \frac{3}{2\pi^2}(\Lambda^4 + \Lambda^2\sigma^2 + \frac{1}{8}\sigma^4) \\ &\quad + \frac{1}{2}\sigma^4 \ln\left(\frac{\sigma}{2\Lambda}\right) \\ &= \left(\frac{1}{4G_S} - \frac{3\Lambda^2}{2\pi^2}\right)\sigma^2 - \frac{3\Lambda^4}{2\pi^2} - \frac{3}{16\pi^2}\sigma^4 \\ &\quad + \frac{3}{4\pi^2}\sigma^4 \ln\frac{2\Lambda}{\sigma}. \end{aligned} \quad (15)$$

The coefficient of σ^2 term, i.e. $(\frac{1}{4G_S} - \frac{3\Lambda^2}{2\pi^2})$, must be negative, since $\sigma = 0$ is a local maximum at QCD vacuum and we can easily verify it by using the fitting parameter value of G_S ($\frac{1}{4G_S} - \frac{3\Lambda^2}{2\pi^2} = -0.0378\Lambda^2$). And when $\sigma/\Lambda \rightarrow \infty$, we have

$$\Omega_{vac}^{H/H'}(\mu_5 = 0) \sim \frac{\sigma^2}{4G_S} - \frac{2\Lambda^3}{\pi^2}\sigma. \quad (16)$$

It is easy to find that the value of σ at the local minimum position, i.e. $\sigma(T = 0) = \sigma_{min} = \frac{4G_S\Lambda^3}{\pi^2}$, is an approximate solution of the gap equation at $T = 0$. And, of course, it is easy to check that this a very rough approximate result, but it reveals the existence of a local minimum solution qualitatively and that $\sigma_{min} \propto G_S$.

When at finite temperature ($\mu_5 = 0$ here), Ω_{th}^H and $\Omega_{th}^{H'}$ will give quite a different result on the transition temperature because of their different cutoff schemes. And we find that T_c obtained by Ω_{th}^H is higher than that obtained by $\Omega_{th}^{H'}$ because of the different upper limits of the integrals. By using the high temperature expansion [45–47] of $\Omega_{th}^{H'}(\mu_5 = 0)$ (when $\sigma \ll T$), we have

$$\begin{aligned} \Omega_{th}^{H'}(\mu_5 = 0) &= -2N_c N_f \left\{ \frac{7\pi^2 T^4}{360} - \frac{T^2 \sigma^2}{24} + \frac{\sigma^4}{16\pi^2} \left[\ln\left(\frac{\pi T}{\sigma}\right) \right. \right. \\ &\quad \left. \left. - \gamma_E + \frac{3}{4} \right] + \mathcal{O}\left(\frac{\sigma^6}{T^2}\right) \right\}, \end{aligned} \quad (17)$$

where $\gamma_E = 0.5772\dots$ is Euler's constant. When $T \rightarrow T_c$, $\sigma \ll T$ and $\sigma \ll \Lambda$, and thus we have

$$\begin{aligned} \Omega_{th}^{H'}(\mu_5 = 0) &= \Omega_{vac}^{H'}(\mu_5 = 0) + \Omega_{th}^{H'}(\mu_5 = 0) \\ &\approx \left[\left(\frac{1}{4G_S} - \frac{3\Lambda^2}{2\pi^2}\right)\sigma^2 - \frac{3\Lambda^4}{2\pi^2} - \frac{3}{16\pi^2}\sigma^4 \right. \\ &\quad \left. + \frac{3}{4\pi^2}\sigma^4 \ln\frac{2\Lambda}{\sigma} \right] - 12 \left\{ \frac{7\pi^2 T^4}{360} - \frac{T^2 \sigma^2}{24} \right. \\ &\quad \left. + \frac{\sigma^4}{16\pi^2} \left[\ln\left(\frac{\pi T}{\sigma}\right) - \gamma_E + \frac{3}{4} \right] \right\}, \\ &= \left(\frac{1}{4G_S} - \frac{3\Lambda^2}{2\pi^2} + \frac{T^2}{2}\right)\sigma^2 - \frac{3\Lambda^4}{2\pi^2} - \frac{7\pi^2 T^4}{30} \\ &\quad - \frac{3\sigma^4}{4\pi^2} \left[\ln\left(\frac{\pi T}{2\Lambda}\right) - \gamma_E + 1 \right]. \end{aligned} \quad (18)$$

When the coefficient of σ^2 term changes the sign from negative to positive as T increases, $\sigma = 0$ point becomes a local minimum and the corresponding temperature could be assumed to be the transition temperature T_c approximately. In this way we obtain $T_c(H') \approx \sqrt{\frac{3\Lambda^2}{\pi^2} - \frac{1}{2G_S}}$ for $\Omega_{th}^{H'}(\mu_5 = 0)$. By using fitting parameters, it is easy to get $T_c(H') = 174.6$ MeV for $\mu_5 = 0$, which is very close to the fully numerical result.

If we use the conventional hard cutoff for the thermal part of potential, i.e. $\Omega_{th}^H(\mu_5 = 0)$, a higher value of T_c will be found.

$$\begin{aligned} \Omega_{th}^H(\mu_5 = 0) &= \Omega_{vac}^H(\mu_5 = 0) + \Omega_{th}^H(\mu_5 = 0) \\ &\approx \left[\left(\frac{1}{4G_S} - \frac{3\Lambda^2}{2\pi^2}\right)\sigma^2 - \frac{3\Lambda^4}{2\pi^2} - \frac{3}{16\pi^2}\sigma^4 \right. \\ &\quad \left. + \frac{3}{4\pi^2}\sigma^4 \ln\frac{2\Lambda}{\sigma} \right] - 12\chi^2(\Lambda) \left\{ \frac{7\pi^2 T^4}{360} - \frac{T^2 \sigma^2}{24} \right. \\ &\quad \left. + \frac{\sigma^4}{16\pi^2} \left[\ln\left(\frac{\pi T}{\sigma}\right) - \gamma_E + \frac{3}{4} \right] \right\}, \\ &= \left(\frac{1}{4G_S} - \frac{3\Lambda^2}{2\pi^2} + \chi^2(\Lambda)\frac{T^2}{2}\right)\sigma^2 - \frac{3\Lambda^4}{2\pi^2} \\ &\quad - \chi^2(\Lambda)\frac{7\pi^2 T^4}{30} - \chi^2(\Lambda)\frac{3\sigma^4}{4\pi^2} \left[\ln\left(\frac{\pi T}{2\Lambda}\right) - \gamma_E + 1 \right]. \end{aligned} \quad (19)$$

where $\chi^2(\Lambda) = \Omega_{th}^H(\mu_5 = 0)/\Omega_{th}^{H'}(\mu_5 = 0)$. Since the integrands of $\Omega_{th}^H(\mu_5 = 0)$ and $\Omega_{th}^{H'}(\mu_5 = 0)$ are the same and positive, $\chi^2(\Lambda) < 1$. Hence, for $\Omega_{th}^H(\mu_5 = 0)$, we get $T_c(H) \approx \frac{1}{\chi(\Lambda)} \sqrt{\frac{3\Lambda^2}{\pi^2} - \frac{1}{2G_S}} > T_c(H')$. Therefore, $T_c(H) > T_c(H')$ at $\mu_5 = 0$ is due to the fact that the conventional cutoff scheme neglects the contribution of the integral from Λ to ∞ in the thermal part of the potential. It will be seen in the next subsection that, when at finite μ_5 , this is also the reason why T_c increases with μ_5 in Ω_{th}^H (when $\mu_5 < 0.4$ GeV actually), while T_c decreases with μ_5 in $\Omega_{th}^{H'}$.

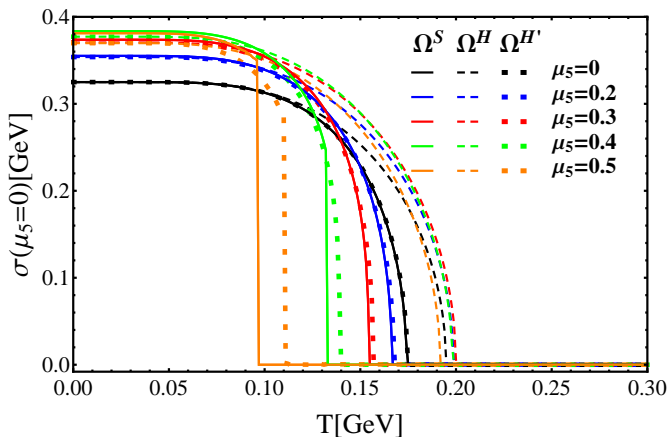


FIG. 2. The dynamical quark mass σ as a function T at $\mu_5 = 0, 0.2, 0.3, 0.4$ and 0.5 for Ω^S, Ω^H and $\Omega^{H'}$.

B. Analysis and Results at $\mu_5 \neq 0$

When μ_5 is introduced, in Fig. 2, we firstly display our numerical results about σ as a function of T at $\mu_5 = 0.2, 0.3, 0.4,$ and 0.5 GeV for three different regularization schemes, comparing with the case at $\mu_5 = 0$. From Fig. 2, we observe that, if μ_5 is not too large (less than 0.4 GeV at least), the chiral condensate increases with μ_5 for all regularization schemes when at zero and low temperatures, which agrees with the result obtained in Refs. [38–44]. But it is no longer valid for Ω^S and $\Omega^{H'}$ when the temperature approaches T_c and this result is just what was found in Refs. [38–40]. And if μ_5 is large enough, we notice that, the chiral condensate at zero temperature begins to decrease with μ_5 and this result has never been found in any previous literature, which will be discussed later. On the other hand, for Ω^S and $\Omega^{H'}$, the effect of μ_5 is to lower the chiral transition temperature, which is exactly the same result in Ref. [38, 40]. As for Ω^H , there exists a critical μ_5^* between 300 MeV and 400 MeV: μ_5 is to raise the critical temperature of the chiral phase transition when $\mu_5 < \mu_5^*$ GeV, which agrees with the result in Ref. [41], while μ_5 turns to decrease the transition temperature when $\mu_5 > \mu_5^*$ GeV, in contrast to the result in Ref. [41].

In addition, we note that, there exists a critical μ_5^c in Ω^S between 300 MeV and 400 MeV, above which the chiral phase transition becomes first-order from second-order, which is just as same as the result in Ref. [38]. And also we find $\Omega^{H'}$ have similar behavior for the order of the chiral phase transition, but its critical μ_5^c is between 400 and 500 MeV. In contrast, the chiral phase transition of Ω^H is always second-order, which is found in Ref. [41]. It indicates that whether there is a change from second-order to first-order above a critical μ_5^c might be due to the choice of the special regularization scheme in the NJL model. And we will not discuss it detailedly in this paper.

Based on above numerical results, now we begin to explore the puzzle that why different regularization schemes

in the NJL model give different effects of μ_5 on the chiral phase transition temperature, especially between $\Omega^H(\mu_5)$ and $\Omega^{H'}(\mu_5)$ (since $\Omega^{H'}(\mu_5)$ and Ω^S have similar results). At $\mu_5 \neq 0$, $\Omega^H(\mu_5)$ and $\Omega^{H'}(\mu_5)$ can be expressed in the following way:

$$\Omega^{H/H'}(\mu_5) = \Omega^{H/H'}(\mu_5 = 0) + \delta\Omega^{H/H'}(\mu_5), \quad (20)$$

where $\delta\Omega^{H/H'}(\mu_5) = \Omega^{H/H'}(\mu_5) - \Omega^{H/H'}(\mu_5 = 0)$, and it can be decomposed into $\delta\Omega_{vac}^{H/H'}(\mu_5) + \delta\Omega_{th}^{H/H'}(\mu_5)$. $\delta\Omega_{vac}^{H/H'}(\mu_5)$ and $\delta\Omega_{th}^{H/H'}(\mu_5)$ contain the effects of the chiral chemical potential μ_5 on the chiral phase transition for the vacuum and the thermal parts, respectively. And we will analyze them analytically and numerically in this paper. In the following, analytical derivations will be given in two feasible scenarios: one is small μ_5 expansion, which is valid at $\mu_5 \ll \sigma$, the other is high-temperature with nonzero μ_5 , which is valid at $\sigma \ll T$ and $\mu_5 \ll T$. Note that μ_5 cannot be too large in both scenarios, and if μ_5 is large enough, the influence of the chiral chemical potential can only be computed and analyzed numerically, which will be shown and discussed in the following also.

1. Small μ_5 expansion

When μ_5 is small enough ($\mu_5 \ll \sigma$), we can expand the thermodynamical potential in powers of μ_5 up to the second order:

$$\Omega = \Omega^{(0)} + \Omega^{(1)} + \Omega^{(2)} + \dots \quad (21)$$

And it is easy to find that $\Omega^{(1)} = 0$, and the nonzero components $\Omega^{(0)}$ and $\Omega^{(2)}$ in hard cutoff and soft cutoff are given as follows, respectively,

$$\Omega^{H/H'(0)} = \Omega_{vac}^{H/H'(0)} + \Omega_{th}^{H/H'(0)}, \quad (22)$$

$$\Omega^{H/H'(2)} = \Omega_{vac}^{H/H'(2)} + \Omega_{th}^{H/H'(2)} \quad (23)$$

with

$$\Omega_{vac}^{H/H'(0)} = \frac{\sigma^2}{4G_S} - N_c N_f \sum_{s=\pm} \int_0^{\Lambda/\Lambda} \frac{dp}{2\pi^2} p^2 \omega_s^{(0)}, \quad (24)$$

$$\Omega_{th}^{H/H'(0)} = -2N_c N_f T \sum_{s=\pm} \int_0^{\Lambda/\infty} \frac{dp}{2\pi^2} p^2 \ln(1 + e^{-\beta\omega_s^{(0)}}), \quad (25)$$

$$\Omega_{vac}^{H/H'(2)} = -\mu_5^2 \sigma^2 \left[N_c N_f \sum_{s=\pm} \int_0^{\Lambda/\Lambda} \frac{dp}{2\pi^2} \frac{p^2}{2(p^2 + \sigma^2)^{3/2}} \right], \quad (26)$$

$$\begin{aligned} \Omega_{th}^{H/H'(2)} = \mu_5^2 N_c N_f \left\{ \sum_{s=\pm} \int_0^{\Lambda/\infty} \frac{dp}{2\pi^2} \left[\frac{\sigma^2}{(1 + e^{\beta\omega_s^{(0)}})} \right. \right. \\ \left. \left. \times \frac{p^2}{(p^2 + \sigma^2)^{3/2}} - \frac{e^{\beta\omega_s^{(0)}}}{(1 + e^{\beta\omega_s^{(0)}})^2} \frac{p^4}{T(p^2 + \sigma^2)} \right] \right\} \quad (27) \end{aligned}$$

and

$$\begin{aligned}\Omega^{S(0)} &= \Omega_{vac}^{S(0)} + \Omega_{th}^{S(0)}, \\ \Omega^{S(2)} &= \Omega_{vac}^{S(2)} + \Omega_{th}^{S(2)}\end{aligned}\quad (28)$$

with

$$\Omega_{vac}^{S(0)} = \frac{\sigma^2}{4G_S} - N_c N_f \sum_{s=\pm} \int_0^\infty \frac{dp}{2\pi^2} f_\Lambda^2(p) p^2 \omega_s^{(0)}, \quad (29)$$

$$\Omega_{th}^{S(0)} = -2N_c N_f T \sum_{s=\pm} \int_0^\infty \frac{dp}{2\pi^2} p^2 \ln(1 + e^{-\beta\omega_s^{(0)}}), \quad (30)$$

$$\Omega_{vac}^{S(2)} = -\mu_5^2 \sigma^2 \left[N_c N_f \sum_{s=\pm} \int_0^\infty \frac{dp}{2\pi^2} f_\Lambda^2(p) \frac{p^2}{2(p^2 + \sigma^2)^{3/2}} \right], \quad (31)$$

$$\begin{aligned}\Omega_{th}^{S(2)} &= \mu_5^2 N_c N_f \left\{ \sum_{s=\pm} \int_0^\infty \frac{dp}{2\pi^2} \left[\frac{\sigma^2}{(1 + e^{\beta\omega_s^{(0)}})} \right. \right. \\ &\quad \left. \left. \times \frac{p^2}{(p^2 + \sigma^2)^{3/2}} - \frac{e^{\beta\omega_s^{(0)}}}{(1 + e^{\beta\omega_s^{(0)}})^2} \frac{p^4}{T(p^2 + \sigma^2)} \right] \right\}\end{aligned}\quad (32)$$

where $\omega_s^{(0)} = \sqrt{\sigma^2 + |\mathbf{p}|^2}$.

At QCD vacuum ($T = 0$), we can obtain from the above equations that the chiral chemical potential μ_5 enhances the coupling constant G_S effectively:

$$\begin{aligned}\frac{1}{4G_S^{eff}(\mu_5)} &= \frac{1}{4G_S} - \mu_5^2 \left[N_c N_f \sum_{s=\pm} \int_0^\Lambda \frac{dp}{2\pi^2} \right. \\ &\quad \left. \times \frac{p^2}{2(p^2 + \sigma^2)^{3/2}} \right] \text{ for } \Omega^H \text{ and } \Omega^{H'},\end{aligned}\quad (33)$$

$$\begin{aligned}\frac{1}{4G_S^{eff}(\mu_5)} &= \frac{1}{4G_S} - \mu_5^2 \left[N_c N_f \sum_{s=\pm} \int_0^\infty \frac{dp}{2\pi^2} \right. \\ &\quad \left. \times f_\Lambda^2(p) \frac{p^2}{2(p^2 + \sigma^2)^{3/2}} \right] \text{ for } \Omega^S,\end{aligned}\quad (34)$$

where $G_S^{eff}(\mu_5)$ is the effective coupling constant for the scalar channel with nonzero μ_5 , which is larger than G_S obviously and increases with μ_5 . Hence, the chiral chemical potential μ_5 contributes to enhance the chiral condensate at zero temperature. From another point of view, when $\sigma \rightarrow 0$, we can find that $\Omega_{vac}^{H/H'(2)}$ helps to increase the magnitude of the coefficient of σ^2 term for $\Omega_{vac}^{H/H'}$, since the coefficient of σ^2 term for $\Omega_{vac}^{H/H'(0)}$ by Eq. (15), i.e. $(\frac{1}{4G_S} - \frac{3\Lambda^2}{2\pi^2})$, is negative. And Ω_{vac}^S can give the same result, since the coefficient of σ^2 term for $\Omega_{vac}^{S(0)}$ must be negative also.

Although the above result is obtained at $\mu_5 \ll \sigma$, we find that it remains valid even when μ_5 is big enough from numerical results. In Fig. 3, we display the potential $\Omega_{vac}(\mu_5; \sigma) - \Omega_{vac}(\mu_5; 0)$ as a function of σ at

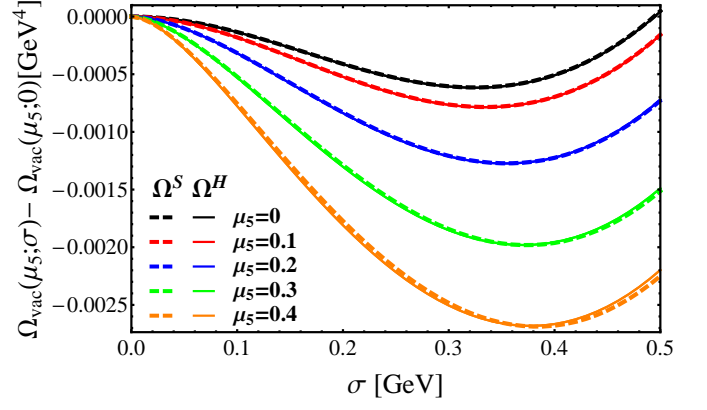


FIG. 3. The potential $\Omega_{vac}(\mu_5; \sigma) - \Omega_{vac}(\mu_5; 0)$ as a function of σ at $\mu_5 = 0, 0.1, 0.2, 0.3$ and 0.4 GeV.

$\mu_5 = 0, 0.1, 0.2, 0.3$ and 0.4 GeV for Ω^S and $\Omega^{H/H'}$ by doing numerical calculations. Obviously, the greater μ_5 values, the faster the curves decrease from the origin. It means that $\delta\Omega_{vac}(\mu_5)$ helps to increase the magnitude of the coefficient of σ^2 term for Ω when $\sigma \rightarrow 0$, which is in agreement with what we get from small μ_5 expansion. In another word, the chiral condensate in the QCD vacuum will increase with μ_5 accordingly, and it is also shown by Fig. 3 that the minimum of the curve shifts to a larger value of σ as μ_5 increases. Thus, $\mu_5 < 0.4$ GeV, increasing μ_5 results in slight enhancement of the chiral condensate at zero temperature, which is verified by the numerical computations and shown in Fig. 4 as well. However, from Fig. 4, we find another interesting phenomenon that there exists a threshold value of μ_5 (μ_5^{thr} is about between 0.4 and 0.5 GeV), above which the quark condensate starts to decrease with μ_5 .

In addition, one can find that the results of the effect of a finite μ_5 on the chiral condensate in the QCD vacuum, by using either Ω_{vac}^S or $\Omega_{vac}^{H/H'}$, agree with each other qualitatively and quantitatively (the difference between them is very small). It is expected that Ω^S and $\Omega^{H'}$ will give consistent results at both zero and finite temperature, since Ω_{th}^S and $\Omega_{th}^{H'}$ have the same expressions. Therefore, in this paper we just need to compare $\Omega^{H'}$ with Ω^H at finite temperature, as mentioned in the previous section, in order to find the reasons for their different effects of μ_5 on chiral transition temperature.

However, at finite temperature, we cannot easily get such a simple result as at zero temperature, because we have to consider the difference between $\delta\Omega_{th}^H(\mu_5)$ and $\delta\Omega_{th}^{H'}(\mu_5)$. Of course, when at low temperatures, it is natural to expect that $\delta\Omega_{vac}(\mu_5)$ will give dominant contribution for either Ω^H or $\Omega^{H'}$, and thus helps to enhance the chiral condensate as μ_5 increases in both regularization schemes, like at zero temperature. When at high temperatures ($T \gtrsim T_c$), it becomes complicated. In the small μ_5 limit, by using $\delta\Omega_{th}^H(\mu_5) = \Omega_{th}^{H(2)} + \dots$ and Eq. 27, one can find that the first term of $\Omega_{th}^{H(2)}$ in Eq. 27

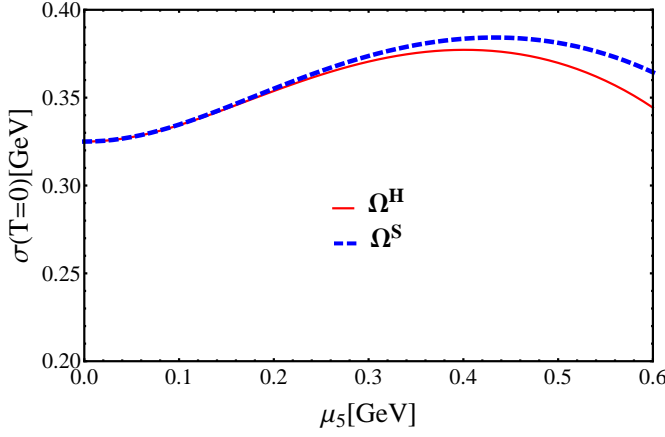
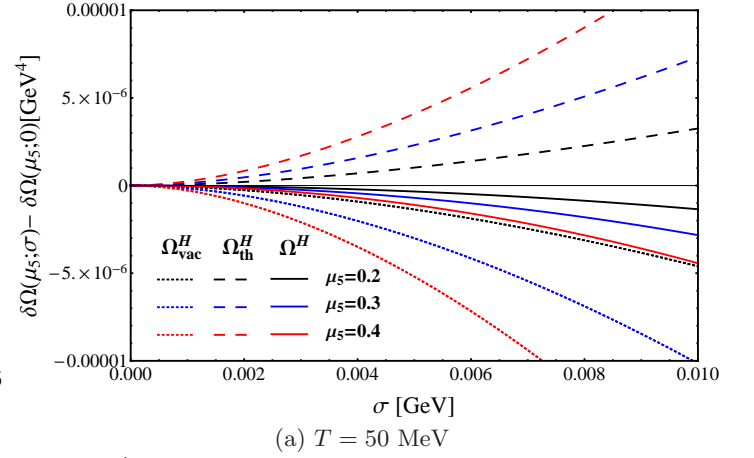


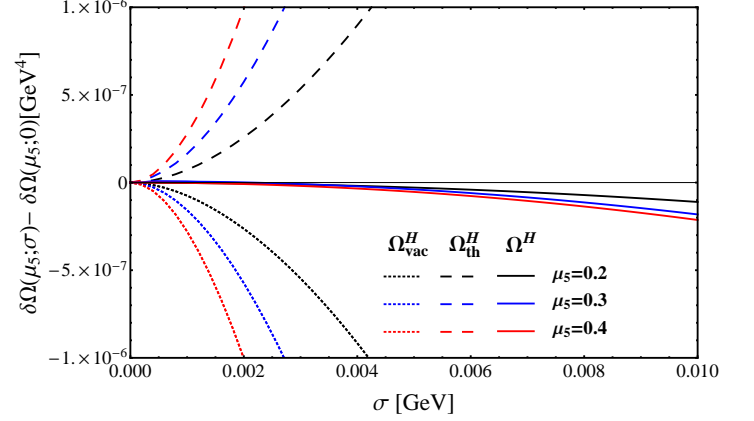
FIG. 4. The chiral condensate at zero temperature as a function of μ_5 for Ω_S and Ω_H (or $\Omega_{H'}$).

makes an opposite contribution to the coefficient of σ^2 term as a result of its positive sign, as compared with $\Omega_{vac}^{H(2)}$ in Eq. 26. Hence, $\Omega_{th}^{H(2)}$ will help to decrease the chiral condensate. Moreover, since $\frac{1}{(1+e^{\beta\omega_s^{(0)}})} < \frac{1}{2}$ at any temperature, the contribution of $\Omega_{th}^{H(2)}$ to the magnitude of the coefficient of σ^2 term is always less than that of $\Omega_{vac}^{H(2)}$. As a consequence, $\Omega^{H(2)}$ helps to increase the chiral condensate at any temperatures, and thus the chiral transition temperature T_c will increase with μ_5 for Ω^H correspondingly in the small μ_5 limit.

And then, we have to resort to numerical calculations to investigate whether this result can be generalized for an arbitrary value of μ_5 ($\mu_5 < \Lambda$ still) by using $\delta\Omega_{th}^H(\mu_5)$. In Fig. 5, we plot the $\delta\Omega_{vac}^H(\mu_5; \sigma) - \delta\Omega_{vac}^H(\mu_5; 0)$, $\delta\Omega_{th}^H(\mu_5; \sigma) - \delta\Omega_{th}^H(\mu_5; 0)$ and $\delta\Omega^H(\mu_5; \sigma) - \delta\Omega^H(\mu_5; 0)$ as a function of σ for $T = 50$ and 170 MeV at $\mu_5 = 0.2, 0.3$ and 0.4 GeV near $\sigma = 0$. From Fig. 5, for $T = 50$ and 170 MeV, one can find that the contribution of $\delta\Omega_{vac}^H$ to the coefficient of σ^2 term is negative, while that of $\delta\Omega_{th}^H$ is positive in contrast. It means that $\delta\Omega_{vac}^H$ helps to increase the chiral condensate, whereas $\delta\Omega_{th}^H$ helps to decrease the chiral condensate, based on previous discussions. And the sum of these two parts, i.e. $\delta\Omega^H = \delta\Omega_{vac}^H + \delta\Omega_{th}^H$, is negative and its magnitude increases with μ_5 . Hence, we find $\delta\Omega^H$ tends to enhance the chiral condensate at any temperatures and the enhancement increases with μ_5 by more detailed numerical calculations, when $\mu_5 < \mu_5^*$ ($0.4 \text{ GeV} < \mu_5^* < 0.5 \text{ GeV}$). And thus we can assume that $\delta\Omega^H$ contribute a term $-b(\mu_5)\sigma^2$, where $b(\mu_5)$ is a positive parameter increasing with μ_5 and $b(\mu_5 = 0) = 0$, to the thermodynamical potential. By using Eq. (19), the coefficient of $\Omega^H(\mu_5) = \Omega^H(\mu_5 = 0) + \delta\Omega^H$ becomes $(\frac{1}{4G_S} - \frac{3\Lambda^2}{2\pi^2} - b(\mu_5)^2 + \chi^2(\Lambda)\frac{T^2}{2})$, so we can obtain the corresponding critical temperature $T_c^H(\mu_5) = \frac{1}{\chi(\Lambda)}\sqrt{(\frac{3\Lambda^2}{\pi^2} + b(\mu_5) - \frac{1}{2G_S})} > T_c^H(\mu_5 = 0)$ and the critical temperature increases with μ_5 under this condition.



(a) $T = 50$ MeV



(b) $T = 170$ MeV

FIG. 5. $\delta\Omega_{vac}^H(\mu_5; \sigma) - \delta\Omega_{vac}^H(\mu_5; 0)$, $\delta\Omega_{th}^H(\mu_5; \sigma) - \delta\Omega_{th}^H(\mu_5; 0)$ and $\delta\Omega^H(\mu_5; \sigma) - \delta\Omega^H(\mu_5; 0)$ as a function of σ for $T = 50$ and 170 MeV at $\mu_5 = 0.2, 0.3$ and 0.4 GeV near $\sigma = 0$

Why the chiral chemical potential turns to reduce the critical temperature when $\mu_5 > \mu_5^*$? We also could find the explanations in Fig. 6, by displaying the $\delta\Omega_{vac}^H(\mu_5; \sigma) - \delta\Omega_{vac}^H(\mu_5; 0)$, $\delta\Omega_{th}^H(\mu_5; \sigma) - \delta\Omega_{th}^H(\mu_5; 0)$ and $\delta\Omega^H(\mu_5; \sigma) - \delta\Omega^H(\mu_5; 0)$ as a function of σ for $T = 200$ MeV at $\mu_5 = 0.2$ and 0.4 GeV near $\sigma = 0$, respectively. Why we choose $T = 200$ MeV? This is because the critical temperatures at $\mu_5 = 0.2$ and 0.4 GeV are close to this value. Obviously, although the contributions of $\delta\Omega^H$ to the coefficient of σ^2 term for both $\mu_5 = 0.2$ and 0.4 GeV are negative, the magnitude of the contribution at $\mu_5 = 0.4$ is smaller than that at $\mu_5 = 0.2$, which is different from the case at lower temperatures. It means that $T_c^H(\mu_5 = 0.2 \text{ GeV})$ and $T_c^H(\mu_5 = 0.4 \text{ GeV})$ are larger than $T_c^H(\mu_5 = 0)$, but $T_c^H(\mu_5 = 0.2 \text{ GeV}) > T_c^H(\mu_5 = 0.4 \text{ GeV})$, if we take similar discussions in the previous paragraph. And it is verified by the numerical simulations that $T_c^H(\mu_5 = 0.2 \text{ GeV}) = 198.7$ MeV, while $T_c^H(\mu_5 = 0.4 \text{ GeV}) = 198.2$ MeV.

As for $\Omega_{th}^{H(2)}$, although it decreases the chiral condensate at finite temperature also, it is not possible to determine whether its contribution is larger than that of

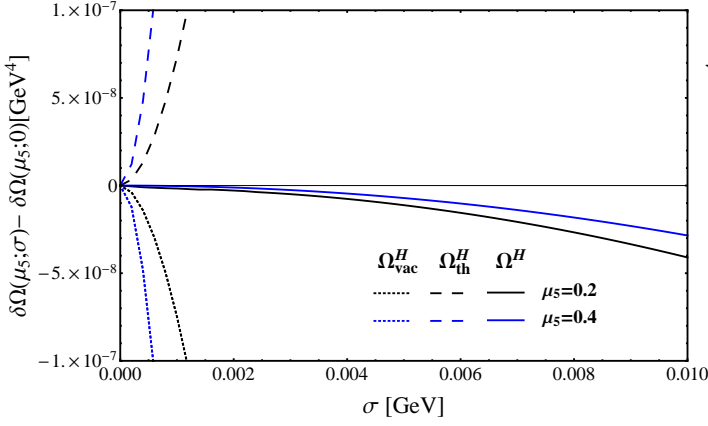


FIG. 6. $\delta\Omega_{vac}^H(\mu_5; \sigma) - \delta\Omega_{vac}^H(\mu_5; 0)$, $\delta\Omega_{th}^H(\mu_5; \sigma) - \delta\Omega_{th}^H(\mu_5; 0)$ and $\delta\Omega^H(\mu_5; \sigma) - \delta\Omega^H(\mu_5; 0)$ as a function of σ for $T = 200$ MeV at $\mu_5 = 0.2$, and 0.4 near $\sigma = 0$

$\Omega_{vac}^{H'(2)}$ around T_c through small μ_5 expansion because of its different upper limit of the integral as compared to $\Omega_{th}^{H(2)}$. But it is find that, by making use of the high-temperature expansion of the thermodynamical potential $\Omega^{H'}$ at finite μ_5 , we reveal the mechanism why μ_5 helps to lower the critical temperature under the regularization scheme of $\Omega^{H'}$ analytically, which is given in the next subsection.

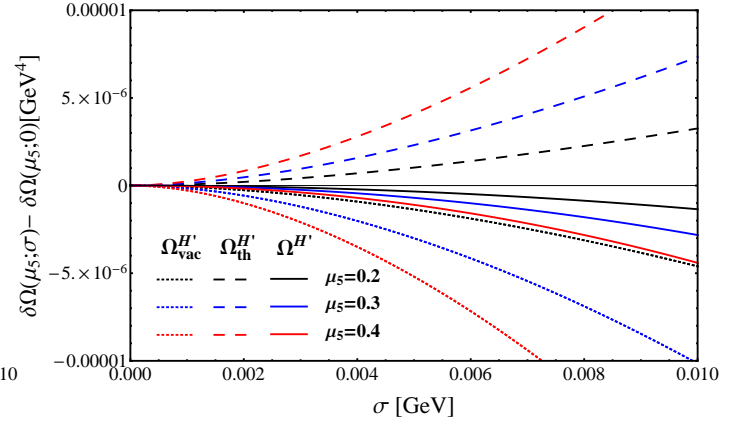
2. High-temperature expansion with nonzero μ_5

Note that the results from $\Omega^{H'}$ are consistent with those from Ω^S , so here we just show the reasons why $\Omega^{H'}$ is different from Ω^H at finite temperature through analytical derivation.

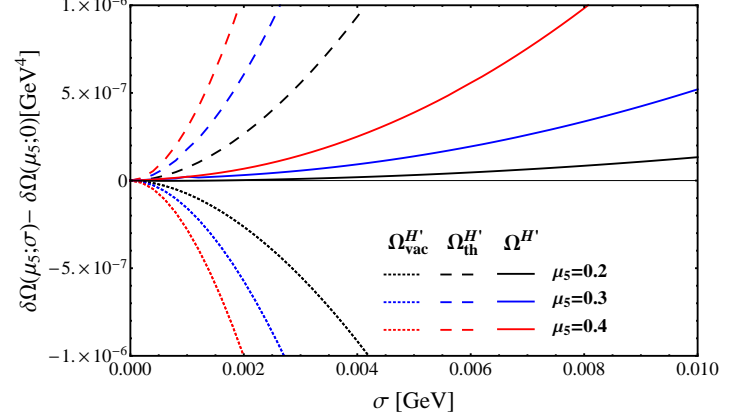
From Eq. 10, we could find that $\Omega_{vac}^{H'}$ takes the exactly same form as Ω_{vac}^H :

$$\begin{aligned} \Omega_{vac}^{H/H'} &= \frac{\sigma^2}{4G_S} - N_c N_f \sum_{s=\pm} \int_0^\Lambda \frac{dp}{2\pi^2} p^2 \omega_s, \\ &= \frac{\sigma^2}{4G_S} - \frac{N_c N_f}{2\pi^2} \times \frac{1}{24} \left\{ \sqrt{(\Lambda + \mu_5)^2 + \sigma^2} \left[2(\Lambda + \mu_5)(3\Lambda^2 - 2\Lambda\mu + \mu_5^2) + (3\Lambda - 13\mu_5)\sigma^2 \right] \right. \\ &\quad + \sqrt{(\Lambda - \mu_5)^2 + \sigma^2} \left[2(\Lambda - \mu_5)(3\Lambda^2 + 2\Lambda\mu + \mu_5^2) \right. \\ &\quad \left. \left. + (3\Lambda + 13\mu_5)\sigma^2 \right] + 6\sigma^2(\sigma^2 - 4\mu_5^2) \right. \\ &\quad \left. \times \ln \left[\frac{\sigma}{2\sqrt{(\Lambda - \mu_5)(\Lambda + \mu_5)}} \right] \right\}. \end{aligned} \quad (35)$$

When T approaches T_c , if we have $\sigma \ll T$ and $\mu_5 \ll T$ (of course, $\sigma \ll \Lambda$ and $\mu_5 \ll \Lambda$ also), we can expand $\Omega_{vac}^{H'}$



(a) $T = 50$ MeV



(b) $T = 170$ MeV

FIG. 7. $\delta\Omega_{vac}^{H'}(\mu_5; \sigma) - \delta\Omega_{vac}^{H'}(\mu_5; 0)$, $\delta\Omega_{th}^{H'}(\mu_5; \sigma) - \delta\Omega_{th}^{H'}(\mu_5; 0)$ and $\delta\Omega^{H'}(\mu_5; \sigma) - \delta\Omega^{H'}(\mu_5; 0)$ as a function of σ for $T = 50$ and 170 MeV at $\mu_5 = 0.2, 0.3$ and 0.4 GeV near $\sigma = 0$

($\Omega_{vac}^{H'}$) in powers of σ/Λ to the second order:

$$\begin{aligned} \Omega_{vac}^{H'} &= \frac{\sigma^2}{4G_S} - \frac{N_c N_f}{2\pi^2} \times \frac{1}{24} \left\{ \frac{6(\Lambda^3 - \Lambda^2\mu_5 - 4\Lambda\mu_5^2 - 2\mu_5^3)}{\Lambda + \mu_5} \right. \\ &\quad \left. + \frac{6(\Lambda^3 + \Lambda^2\mu_5 - 4\Lambda\mu_5^2 + 2\mu_5^3)}{\Lambda - \mu_5} - 24\mu_5^2 \right. \\ &\quad \left. \times \ln \left[\frac{\sigma}{2\sqrt{(\Lambda - \mu_5)(\Lambda + \mu_5)}} \right] \right\} \sigma^2 + \dots \end{aligned} \quad (36)$$

Thus, with considering $\mu_5 \ll \Lambda$, we get in the $\sigma \rightarrow 0$ limit:

$$\delta\Omega_{vac}^{H'}(\mu_5; \sigma) - \delta\Omega_{vac}^{H'}(\mu_5; 0) = \frac{N_c N_f}{2\pi^2} \times \mu_5^2 \left(\ln \frac{\sigma}{2\Lambda} + 1 \right) \sigma^2. \quad (37)$$

Since $(\ln \frac{\sigma}{2\Lambda} + 1)$ is negative near T_c , the contribution of $\delta\Omega_{vac}^{H'}$ to the coefficient of σ^2 term is negative near $\sigma = 0$, which helps to increase the chiral condensate.

As for the thermal part, we have

$$\Omega_{th}^{H'} = -2N_c N_f T \sum_{s=\pm} \int_0^\infty \frac{dp}{2\pi^2} p^2 \ln(1 + e^{-\beta\omega_s}). \quad (38)$$

When at high temperatures ($\sigma \ll T$ and $\mu_5 \ll T$), we can expand $\Omega_{th}^{H'}$ as follows (we use the same strategy in Refs. [45–47]):

$$\begin{aligned} \Omega_{th}^{H'} = & -2N_c N_f \left\{ \left(\frac{\mu_5^2}{12} - \frac{\sigma^2}{24} \right) T^2 + \frac{\sigma^4}{16\pi^2} \left[\ln\left(\frac{\pi T}{\sigma}\right) - \gamma_E + \frac{3}{4} \right] \right. \\ & + \frac{1}{4\pi^2} \left[\gamma_E - \frac{1}{2} - \ln\left(\frac{\pi T}{\sigma}\right) \right] \mu_5^2 \sigma^2 + \frac{7\pi^2 T^4}{360} \\ & \left. + \mathcal{O}\left(\frac{\sigma^6}{T^2}, \frac{\sigma^4 \mu_5^2}{T^2}\right) \right\}, \quad (39) \end{aligned}$$

Similar to $\Omega_{vac}^{H'}$, in the $\sigma \rightarrow 0$ limit, we obtain

$$\begin{aligned} \delta\Omega_{th}^{H'}(\mu_5; \sigma) - \delta\Omega_{th}^{H'}(\mu_5; 0) = & \frac{N_c N_f}{2\pi^2} \left[\ln\left(\frac{\pi T}{\sigma}\right) - \gamma_E \right. \\ & \left. + \frac{1}{2} \right] \mu_5^2 \sigma^2. \quad (40) \end{aligned}$$

Since $T \gg \sigma$ near T_c , the contribution of the thermal part to the coefficient of σ^2 term is positive near $\sigma = 0$ and it helps to decrease the chiral condensate.

And then, combining Eq. (40) with Eq. (37), we can find that

$$\begin{aligned} \delta\Omega^{H'}(\mu_5; \sigma) - \delta\Omega^{H'}(\mu_5; 0) = & \frac{N_c N_f}{2\pi^2} \left[\ln\left(\frac{\pi T}{2\Lambda}\right) - \gamma_E \right. \\ & \left. + \frac{3}{2} \right] \mu_5^2 \sigma^2. \quad (41) \end{aligned}$$

When T is large enough, its coefficient of σ^2 term will become positive from negative. It indicates that, when at low temperatures, $\delta\Omega^{H'}$ helps to increase the chiral condensate, whereas when at enough high temperatures, this will make a change and $\delta\Omega^{H'}$ helps to decrease the chiral condensate. Moreover, from Eq. (41), the magnitude of the coefficient will increase with μ_5 when at enough high temperatures and it means the critical temperature will decrease with μ_5 by taking the analysis similar to $\delta\Omega^H$. Assuming $T_c = T_c^0 + \delta T$ at small μ_5 , where $T_c^0 = T_c(\mu_5 = 0)$, we can find δT satisfies

$$\left(\frac{1}{4G_S} - \frac{3\Lambda^2}{2\pi^2} + \frac{T_c^2}{2} \right) + \frac{N_c N_f}{2\pi^2} \left[\ln\left(\frac{\pi T_c}{2\Lambda}\right) - \gamma_E + \frac{3}{2} \right] \mu_5^2 = 0, \quad (42)$$

and then we have $\delta T = -\frac{3\mu_5^2}{\pi^2(T_c^0)^2} \left[\ln\left(\frac{\pi T_c^0}{2\Lambda}\right) - \gamma_E + \frac{3}{2} \right] T_c^0 < 0$, since it is to check $\ln\left(\frac{\pi T_c^0}{2\Lambda}\right) - \gamma_E + \frac{3}{2} > 0$. This result was also obtained in Ref. [40].

In order to investigate the validity of our analysis at relatively large μ_5 values, we resort to numerical computations to plot $\delta\Omega_{vac}^{H'}(\mu_5; \sigma) - \delta\Omega_{vac}^{H'}(\mu_5; 0)$, $\delta\Omega_{th}^{H'}(\mu_5; \sigma) - \delta\Omega_{th}^{H'}(\mu_5; 0)$ and $\delta\Omega^{H'}(\mu_5; \sigma) - \delta\Omega^{H'}(\mu_5; 0)$ as a function

of σ for $T = 50$ and 170 MeV at $\mu_5 = 0.2, 0.3$ and 0.4 GeV near $\sigma = 0$ in Fig. 7. From Fig. 7, we notice that, when $T = 50$ MeV (a low temperature), the sum of the vacuum and thermal parts, $\delta\Omega^H$, is negative and the magnitude of the coefficient of the σ^2 term increase with μ_5 . Hence, we can conclude that the chiral condensate make an enhancement as μ_5 increases. When at $T = 170$ MeV (close to $T_c^{H'}(\mu_5 = 0)$), it is obvious that the contribution of $\delta\Omega^H$ to the coefficient of the σ^2 becomes positive and its magnitude increases with μ_5 also. Consequently, the critical temperature will decrease with μ_5 .

IV. CONCLUSIONS

In this paper, we have studied the effects of the chiral chemical potential μ_5 on the chiral phase transition for three different regularization schemes in the NJL model. Based on the analytical and numerical analysis of the thermodynamical potential Ω , we find that the coefficient of σ^2 term for the potential Ω reflects the behavior of the chiral condensate and the critical temperature. Thus, we compare the modifications of the coefficients of σ^2 terms made by μ_5 , for the thermodynamical potentials in three regularization schemes, i.e. Ω^S , Ω^H and $\Omega^{H'}$. In this way, we have found the reason for the puzzle that why the same NJL model in Refs. [38, 40] and [41], due to the choice of the regularization scheme, gave two opposite results about the dependence of the critical temperature on μ_5 totally distinct from each other. This is because the conventional hard-cutoff regularization scheme includes a hard cutoff function $\theta(\Lambda - |\mathbf{p}|)$ for the thermal part of the thermodynamical potential, so that its thermal part Ω_{th}^H does not contain all the contribution from the chiral chemical potential μ_5 . In fact, the thermal part of the thermodynamical potential is convergent, so there is no need to introduce any cutoff function for it at all. Therefore, the results obtained from the soft-cutoff and revised hard-cutoff regularization schemes are more reasonable.

In our study, we have first investigated the effect of the chiral chemical potential on the chiral condensate for the vacuum part and the thermal part of the thermodynamical potential, respectively. Our results show a competition between these two parts that, the vacuum part tends to increase the chiral condensate, while the thermal part tends to decrease the chiral condensate. Relying on both analytical analysis of the small μ_5 expansion and numerical computations, it is found that at zero and low temperatures, if $m\mu_5 < m\mu_5^{thr}$, the contribution of the vacuum part is greater than that of the thermal part for all three regularization schemes, so that the chiral chemical potential catalyze the chiral symmetry breaking, which is consistent with the result of all previous Refs. [38–44]. When at high temperatures around T_c , different regularization schemes give two different results. For Ω^H , perturbative expansion in the small μ_5 limit, as well as numerical calculations, explicitly tells us the contribu-

tion of the thermal term is always less than that of the vacuum term at any temperatures because of its regularization scheme, which is also verified by the numerical results for $\mu_5 < \mu_5^*$. As for Ω^S and $\Omega^{H'}$, the numerical calculations show us that the contribution of the thermal term will exceed that of the vacuum term when the temperature is high enough. Moreover, we should mention that, even at zero temperature, the dependence of the chiral condensate as a function of μ_5 is not monotonically increasing, which is different from all previous results. When $\mu_5 > \mu_5^*$, the quark condensate turns to decrease with μ_5 , although its value is still larger than that in the vacuum.

We have also computed the effect of the chiral chemical potential on the chiral critical temperature. On the basis of the discussions about the corrections of μ_5 on the coefficient of σ^2 term for the potential Ω , we find that, for Ω^H , the critical temperature T_c increases with μ_5 when $\mu_5 < \mu_5^*$, while T_c decreases with μ_5 when $\mu_5 > \mu_5^*$. The latter is not in agreement with the result in Ref. [41], and this is because that in Ref. [41], its maximum value of μ_5 is just 0.5Λ and less than μ_5^* . Depending on the similar analysis, we obtain that the critical temperature is always decreasing function of μ_5 for Ω^S and $\Omega^{H'}$. Therefore, for the conventional hard-cutoff regularization scheme, its increasing behavior of the critical temperature as a

function of the chiral chemical potential is caused by the incomplete contribution of the thermal part.

In the future, it is important to extend our analysis to the 2 + 1 flavors and take into account the effect of finite current quark mass. On the other hand, it is of interest to explore the underlying reasons for the order of the chiral phase transition with finite chiral chemical potential in the NJL model with different regularization schemes. Moreover, why the behavior of the critical temperature in both the NJL model [38, 40] and some other effective models [39] is different from that in DSEs [43] and lattice QCD [44] is still an open question. How to choose a proper regularization scheme may play an important role.

ACKNOWLEDGEMENT

We thank valuable discussions with M. Chernodub and T. Kojo. This work is supported by the NSFC under Grant No. 11275213, and 11261130311(CRC 110 by DFG and NSFC), CAS key project under Grant No. KJCX2-EW-N01, and the Youth Innovation Promotion Association of CAS. L.Yu is partially supported by China Postdoctoral Science Foundation under Grant No. 2014M550841 and the Seeds Funding of Jilin University.

-
- [1] A. A. Belavin, A. M. Polyakov, A. S. Schwartz and Y. S. Tyupkin, Phys. Lett. B **59**, 85 (1975).
 [2] G. 't Hooft, Phys. Rev. Lett. **37**, 8 (1976).
 [3] G. 't Hooft, Phys. Rev. D **14**, 3432 (1976) [Phys. Rev. D **18**, 2199 (1978)].
 [4] T. Schäfer and E. V. Shuryak, Rev. Mod. Phys. **70**, 323 (1998) [hep-ph/9610451].
 [5] E. Witten, Nucl. Phys. B **156**, 269 (1979).
 [6] G. Veneziano, Nucl. Phys. B **159**, 213 (1979).
 [7] N. S. Manton, Phys. Rev. D **28**, 2019 (1983).
 [8] F. R. Klinkhamer and N. S. Manton, Phys. Rev. D **30**, 2212 (1984).
 [9] V. A. Kuzmin, V. A. Rubakov and M. E. Shaposhnikov, Phys. Lett. B **155**, 36 (1985).
 [10] P. B. Arnold and L. D. McLerran, Phys. Rev. D **36**, 581 (1987).
 [11] S. Y. Khlebnikov and M. E. Shaposhnikov, Nucl. Phys. B **308**, 885 (1988).
 [12] P. B. Arnold and L. D. McLerran, Phys. Rev. D **37**, 1020 (1988).
 [13] L. D. McLerran, E. Mottola and M. E. Shaposhnikov, Phys. Rev. D **43**, 2027 (1991).
 [14] G. D. Moore, Phys. Lett. B **412**, 359 (1997) [hep-ph/9705248].
 [15] G. D. Moore and K. Rummukainen, Phys. Rev. D **61**, 105008 (2000) [hep-ph/9906259].
 [16] D. Bodeker, G. D. Moore and K. Rummukainen, Phys. Rev. D **61**, 056003 (2000) [hep-ph/9907545].
 [17] G. D. Moore, hep-ph/0009161.
 [18] V. Skokov, A. Y. Illarionov and V. Toneev, Int. J. Mod. Phys. A **24**, 5925 (2009) [arXiv:0907.1396 [nucl-th]].
 [19] V. Voronyuk, V. D. Toneev, W. Cassing, E. L. Bratkovskaya, V. P. Konchakovski and S. A. Voloshin, Phys. Rev. C **83**, 054911 (2011) [arXiv:1103.4239 [nucl-th]].
 [20] A. Bzdak and V. Skokov, Phys. Lett. B **710**, 171 (2012) [arXiv:1111.1949 [hep-ph]].
 [21] W. -T. Deng and X. -G. Huang, Phys. Rev. C **85**, 044907 (2012) [arXiv:1201.5108 [nucl-th]].
 [22] D. E. Kharzeev, L. D. McLerran and H. J. Warringa, Nucl. Phys. A **803**, 227 (2008) [arXiv:0711.0950 [hep-ph]].
 [23] K. Fukushima, D. E. Kharzeev and H. J. Warringa, Phys. Rev. D **78**, 074033 (2008) [arXiv:0808.3382 [hep-ph]].
 [24] K. Fukushima, M. Ruggieri and R. Gatto, Phys. Rev. D **81**, 114031 (2010) [arXiv:1003.0047 [hep-ph]].
 [25] B. I. Abelev *et al.* [STAR Collaboration], Phys. Rev. Lett. **103**, 251601 (2009) [arXiv:0909.1739 [nucl-ex]].
 [26] B. I. Abelev *et al.* [STAR Collaboration], Phys. Rev. C **81**, 054908 (2010).
 [27] B. Abelev *et al.* [ALICE Collaboration], Phys. Rev. Lett. **110**, 012301 (2013).
 [28] S. P. Klevansky and R. H. Lemmer, Phys. Rev. D **39**, 3478 (1989).
 [29] K. G. Klimenko, Theor. Math. Phys. **89**, 1161 (1992) [Teor. Mat. Fiz. **89**, 211 (1991)].
 [30] V. P. Gusynin, V. A. Miransky and I. A. Shovkovy, Nucl. Phys. B **462**, 249 (1996) [hep-ph/9509320].
 [31] G. S. Bali, F. Bruckmann, G. Endrodi, Z. Fodor, S. D. Katz, S. Krieg, A. Schafer and K. K. Szabo, JHEP **1202**, 044 (2012) [arXiv:1111.4956 [hep-lat]].

- [32] G. S. Bali, F. Bruckmann, G. Endrodi, Z. Fodor, S. D. Katz and A. Schafer, *Phys. Rev. D* **86**, 071502 (2012) [arXiv:1206.4205 [hep-lat]].
- [33] M. N. Chernodub, *Phys. Rev. D* **82**, 085011 (2010) [arXiv:1008.1055 [hep-ph]].
- [34] M. N. Chernodub, *Phys. Rev. Lett.* **106**, 142003 (2011) [arXiv:1101.0117 [hep-ph]].
- [35] J. Chao, P. Chu and M. Huang, *Phys. Rev. D* **88**, 054009 (2013) [arXiv:1305.1100 [hep-ph]].
- [36] L. Yu, H. Liu and M. Huang, *Phys. Rev. D* **90**, no. 7, 074009 (2014) [arXiv:1404.6969 [hep-ph]].
- [37] L. Yu, J. Van Doorselaere and M. Huang, *Phys. Rev. D* **91**, no. 7, 074011 (2015) [arXiv:1411.7552 [hep-ph]].
- [38] K. Fukushima, M. Ruggieri and R. Gatto, *Phys. Rev. D* **81**, 114031 (2010) [arXiv:1003.0047 [hep-ph]].
- [39] M. N. Chernodub and A. S. Nedelin, *Phys. Rev. D* **83**, 105008 (2011) [arXiv:1102.0188 [hep-ph]].
- [40] R. Gatto and M. Ruggieri, *Phys. Rev. D* **85**, 054013 (2012) [arXiv:1110.4904 [hep-ph]].
- [41] Gaoqing Cao, PhD thesis from Tsinghua University (2015).
- [42] B. Wang, Y. L. Wang, Z. F. Cui and H. S. Zong, *Phys. Rev. D* **91**, no. 3, 034017 (2015). [43]
- [43] S. S. Xu, Z. F. Cui, B. Wang, Y. M. Shi, Y. C. Yang and H. S. Zong, *Phys. Rev. D* **91**, no. 5, 056003 (2015) [arXiv:1505.00316 [hep-ph]].
- [44] V. V. Braguta, E.-M. Ilgenfritz, A. Y. Kotov, M. Mller-Preussker, B. Petersson and A. Schreiber, *PoS LATTICE* **2014**, 235 (2015) [arXiv:1411.5174 [hep-lat]].
- [45] L. Dolan and R. Jackiw, *Phys. Rev. D* **9**, 3320 (1974).
- [46] H. E. Haber and H. A. Weldon, *Phys. Rev. Lett.* **46**, 1497 (1981).
- [47] H. E. Haber and H. A. Weldon, *J. Math. Phys.* **23**, 1852 (1982).